Proceedings of the 4th International Conference on Functional Materials and Civil Engineering
DOI: 10.54254/2755-2721/2026.38751

Interface Pressure Optimization for a Lower Limb Assistive Exoskeleton—Mechanical Modeling and Monte Carlo Simulation of Segmented Compliant Supports

Dongze Li

Xi'an Gaoxin No. 1 High School, Xi'an, China
18700877012@163.com

Abstract. The effect of the straps and support structures of a lower limb gait assist exoskeleton on pressure at the skin and soft tissue interface is examined. Because muscle atrophy may alter how loads pass between the limb and the device, a quasi-static torque and contact model for a lateral knee support model was developed. The nominal model used an assistive torque of 8 N·m and a support spacing of 0.24 m. A narrow circumferential cuff, a wide circumferential cuff, and segmented compliant pads were compared using the Markov Chain Monte Carlo method. Assistive torque, support spacing, effective contact fraction, strap preload, and a local concentration factor were varied. Under the stated model assumptions, the segmented pad concept had a median mean pressure of 8.9 kPa, with a 95% simulation interval of 6.8 to 11.5 kPa. Its peak pressure proxy had a median of 11.7 kPa, with an interval of 8.5 to 16.1 kPa. The corresponding medians for the narrow cuff were 20.6 and 36.9 kPa. Based on the comparison, an open, segmented load-bearing pad is proposed and bench testing on a limb surrogate is recommended. In the future, this study has implications on wearable pressure limits for older adults.

Keywords: lower limb exoskeleton, human-device interface, interface pressure, muscle atrophy, Monte Carlo simulation

1. Introduction

Lower limb exoskeletons and exosuits transmit joint torque through the interface between the wearer and the device. The interface also produces normal pressure, shear, tissue deformation, and relative motion. Previous work has measured pressure distributions at exoskeleton contact surfaces, monitored dynamic strap pressure, and assessed human-exoskeleton interaction mechanics [1-4]. Differences in device structure, sensors, tasks, and outcome measures still make results across studies difficult to compare directly [3, 4].

The fit and loading concerns raised for older adults with muscle atrophy or long-term mobility limitations, particularly the loads straps may place on skin, soft tissue, and bone, are focused on. Reduced muscle thickness may alter the path through which loads are transmitted, while osteoporosis can increase fracture risk. Interface pressure cannot be converted directly into fracture risk. Fracture also depends on bone strength, loading direction, joint posture, and events such as falls

© 2026 The Authors. This is an open access article distributed under the terms of the Creative Commons Attribution License 4.0 (https://creativecommons.org/licenses/by/4.0/).

DOI: 10.54254/2755-2721/2026.38751

or impacts, so p = F/A alone is not a clinical measure. The concern is therefore framed as an engineering question: while delivering the required support torque, how can a design limit local pressure peaks and avoid unnecessary strap preload?

Evidence on cuff width and comfort depends on the conditions under which pressure is applied. In a walking compression study of 21 healthy participants, Kermavnar et al. found that discomfort or pain occurred at lower pressures during walking than during quiet standing, with outcomes also varying by anatomical site, compression method, and cuff width [5]. They discussed force application sites, cuff width, and inflation pressure for soft exoskeletons. Because those recommendations came from healthy participants and a specific cuff experiment, their use with older adults with muscle atrophy requires dedicated validation. A review of people with chronic pain also reported that some participants experienced pain within a range of about 10 to 18 kPa [6]. 14 kPa is used as a literature reference line, not as a product acceptance criterion. To address this question, assistive torque is converted to interface reaction force and then contact pressure is estimated. Mean pressure, local concentration, and retention strap preload are examined separately, and three structural concepts are compared using a fixed random seed. A product concept for future fabrication and bench testing is concluded with. The present work is limited to modeling and simulation. Prototype and clinical evaluation remain for future study.

The design concepts have been implemented by some studies in the literature. De Rossi et al. developed a distributed pressure sensor made from soft silicone and placed it between a lower limb rehabilitation robot and the wearer to measure contact pressure and calibrate load [1]. Tamez-Duque et al. proposed a real-time strap pressure monitoring system for powered exoskeletons and conducted an initial evaluation with two participants. They reported that pressure could differ substantially across locations on the same strap [2]. Armitage et al. reviewed interface pressure measurement in prosthetic, orthotic, and exoskeleton applications, including normal and shear sensing, calibration, and comparisons across devices [7]. This work supports the use of pressure maps and spatial measures alongside an average value. Massardi et al. reviewed methods for evaluating human-exoskeleton interaction dynamics. They noted that pressure, force, torque, relative motion, and physiological responses need to be interpreted in relation to the task, and that a unified evaluation procedure remains to be established [3]. Kermavnar et al. examined the relation between pneumatic cuff inflation and limb interface pressure, showing that limb dimensions and cuff parameters affect pressure transmission [8]. The pressure maps are therefore treated as conceptual simulation outputs. A prototype would require recalibration for sensor sensitivity, spatial resolution, and installation on a curved surface.

In addition, Sanchez-Villamañan et al. proposed the design of compliant lower limb exoskeletons, covering actuators, structural compliance, and attachment methods, and emphasizing wearer fit and compensation for joint misalignment [9]. Kermavnar et al. found that sustained and phase-dependent compression may affect deep tissue oxygenation differently, and that pressure tolerance varies with body site and dynamic task [5]. Another study linked discomfort to changes in soft tissue volume and oxygenation [10]. Together, these findings suggest that a wider continuous cuff may lower a model's average pressure without necessarily improving a wearer's experience. Bessler et al. argued that safety assessment for rehabilitation robots should cover mechanical, electrical, control, environmental, and patient-related hazards throughout design and verification [11]. ISO/TR 23482-1:2020 provides test methods related to the safety requirements for personal care robots. Whether ISO 13482 applies depends on the device's intended use and regulatory pathway [12]. In light of this work, our product concept includes rapid unloading, force limitation, pressure monitoring, and

DOI: 10.54254/2755-2721/2026.38751

bench testing. Simulation supports early design screening, while safety certification and clinical evaluation must follow the product development process.

2. Methods

2.1. Design object and force model

A concept for a passive lateral knee support frame that transfers load through thigh and shank interfaces is studied. The sagittal-plane assistive torque supplied by the exoskeleton is denoted as M and the distance between the two interface reaction forces as d. Under a quasi-static force-couple approximation, the reaction force required at each interface is given by Equation (1). For the nominal case, M = 8 N·m and d = 0.24 m, giving an interface force of 33.3 N. This relation provides a first-order load estimate. Soft tissue deformation, joint friction, hinge-axis offset, gait acceleration, and voluntary muscle force are treated within the simplifying assumptions of the model. The ranges of M and d define design scenarios for this study.

The effective contact area is calculated using Equation (2) and mean interface pressure is estimated with Equation (3). Here, w is pad width along the limb, L is contact arc length, φ is the fraction of the nominal area that carries load, and p_0 is the preload pressure used to keep the device in contact with the limb. Pressure is reported in kPa, with F in newtons and A_{eff} in square metres. The assistive reaction and retention strap preload are kept separate so that functional loading can be distinguished from positioning load. Equation (4) estimates a local peak pressure proxy, where K represents the combined effects of edge concentration, limb curvature, and load offset.

A normalized spatial pressure field is generated using Equation (5), with the area average of q(x,y) over the contact region set to one. The simulated field for Concept A includes edge and unilateral loading peaks. Concept B reduces the edge peak while retaining a circumferential preload. Concept C uses two segmented compliant load-bearing pads, leaves clearance over the front of the knee, and reduces retention strap preload. The three q fields follow the assumptions stated here and serve as conceptual distributions for comparison.

$$F = M/d \tag{1}$$

$$A_{eff} = w\,L\,\varphi \tag{2}$$

$$\bar{p} = F/(1000A_{eff}) + p_0 \tag{3}$$

$$\hat{p} = K\bar{p} \tag{4}$$

$$p(x,y) = p_0 + [F/(1000A_{eff})]q(x,y), \quad \langle q \rangle_a = 1 \tag{5}$$

2.2. Concepts and parameters

Three interface concepts are compared. Concept A is a narrow circumferential cuff, 35 mm wide with a contact arc length of 110 mm. Concept B is a wide circumferential cuff, 65 mm wide with the same contact arc length. Concept C uses segmented compliant support pads with a projected load-bearing width of 58 mm, an effective arc length of 105 mm, and an open retention strap. For Concept C, the stated width is the total projected width of the pads rather than a continuous cuff around the limb. The effective contact fraction φ is used to adjust the geometric area. Table 1 lists the simulation parameters.

DOI: 10.54254/2755-2721/2026.38751

Table 1. Structural concepts and model parameters used in this study. All values are design assumptions, and no individual anthropometric measurements were used

Parameter	A Narrow cuff	B Wide cuff	C Segmented pads
Nominal pad width w (mm)	35	65	58
Contact length L (mm)	110	110	105
Effective contact fraction φ (mean ± SD)	0.60 ± 0.08	0.73 ± 0.07	0.86 ± 0.05
Preload pressure p_0 (kPa, mean)	6.0	4.5	2.5
Concentration factor K (mean ± SD)	1.80 ± 0.22	1.55 ± 0.18	1.32 ± 0.13

2.3. Monte Carlo simulation and summary statistics

NumPy's random number generator was used with the seed fixed at 20260923 and 10,000 trials were run for each concept. In each trial, M was drawn from a uniform distribution between 6 and 10 N·m and d from a uniform distribution between 0.20 and 0.28 m. φ and K were sampled from the normal distributions in Table 1 and clipped to physically feasible ranges. The standard deviation of p_0 was set to 12% of its mean, with negative values set to zero.

Interface force, effective area, mean pressure, and the peak proxy were then calculated using Equations (1) through (4). The results are summarized using medians, 2.5th to 97.5th percentile intervals, and the fraction of peak proxy values above the 14 kPa reference. This fraction describes how often model outputs exceed the literature reference and supports comparisons among concepts.

The same draws of M and d were used for all three concepts so that changes in these common inputs could be compared directly. φ, K, and p_0 were sampled separately for each concept. Because the model samples these parameters independently, the resulting intervals describe design uncertainty under our assumptions.

2.4. Design evaluation measures

The concepts are compared using four measures: mean pressure $\bar{p}$, local peak proxy $\hat{p}$, the fraction of simulations above the 14 kPa reference, and the effect of each interface concept on device function. The last measure is assessed qualitatively in terms of load transfer, joint alignment, donning and doffing, cleaning, and rapid release. These factors are reported separately to inform later design choices and risk assessment. The simulation aims to reduce the high-pressure tail while retaining stable load transfer. Each candidate structure will also require slip and shear testing.

3. Results

3.1. Nominal contact pressure fields

For the nominal case, the force-couple reaction is 33.3 N. Using the mean contact fractions in Table 1 gives different average pressures across the three concepts. Figure 1 also shows that similar average pressures can conceal different edge concentrations and off-center loading. The simulated fields are displayed in grayscale. Peak locations arise from the edge concentration functions specified in the model, so Figure 1 compares modeling assumptions rather than pressure measurements from a wearer.

DOI: 10.54254/2755-2721/2026.38751

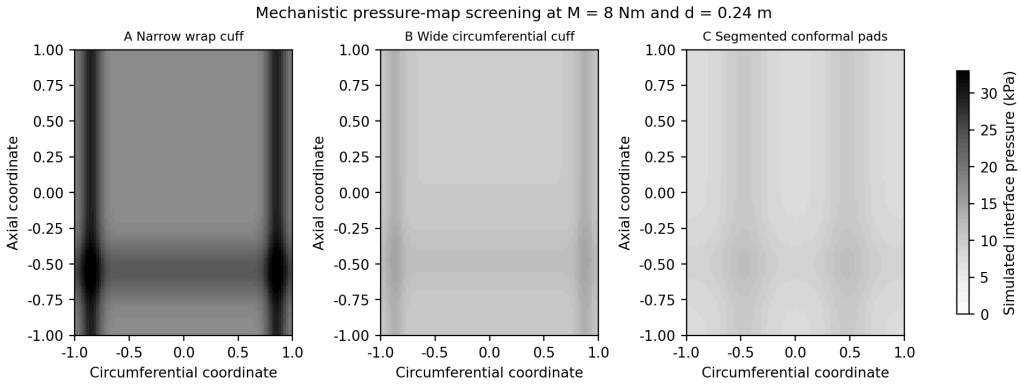


Figure 1. Simulated pressure distributions for the three interface concepts at M = 8 N·m and d = 0.24 m. Grayscale indicates pressure in kPa. The plotted values were generated from the model parameters used in this study

3.2. Uncertainty propagation

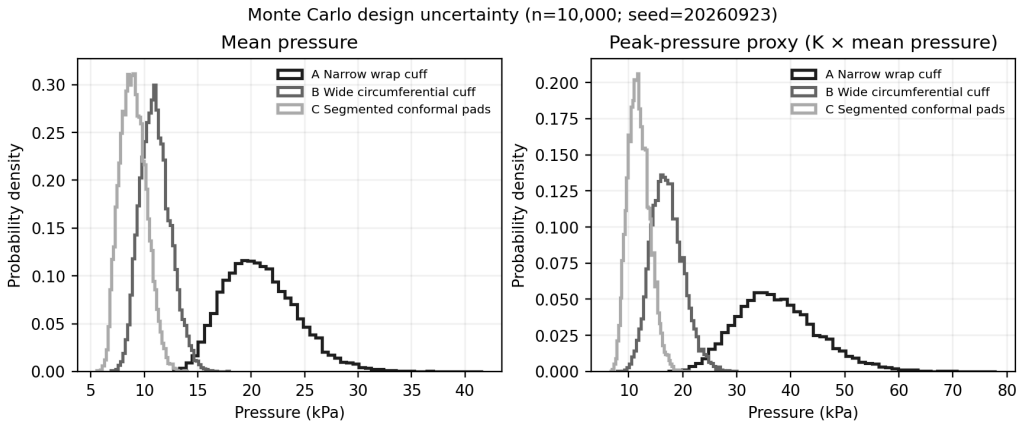


Figure 2. Distributions of simulated mean pressure and peak pressure proxy from 10,000 Monte Carlo trials. All plotted values are simulation samples

For the narrow cuff, median mean pressure was 20.56 kPa, with a 95% simulation interval of 15.28 to 28.36 kPa. The median peak proxy was 36.88 kPa, with an interval of 24.60 to 54.83 kPa. Every simulated peak proxy exceeded the 14 kPa literature reference. For the wide cuff, median mean pressure was 10.93 kPa, with a 95% simulation interval of 8.57 to 14.06 kPa. The median peak proxy was 16.90 kPa, with an interval of 11.84 to 23.55 kPa. The peak proxy exceeded the 14 kPa reference in 85.5% of trials. For the segmented compliant pads, median mean pressure was 8.90 kPa, with a 95% simulation interval of 6.85 to 11.47 kPa. The median peak proxy was 11.69 kPa, with an interval of 8.51 to 16.06 kPa. The peak proxy exceeded the reference in 14.9% of trials. Under the assumptions used here, the segmented concept combines lower retention preload with a higher estimated effective contact fraction. Its simulated mean pressure and peak proxy are therefore lower than those of the other two concepts. This difference follows from the model inputs and represents a relative change across simulated designs. In practice, performance will also depend on pad fit, load path, and limb circumference. If the open structure slips, the reaction may become concentrated again near a smaller edge region. The distributions of simulated mean pressure and

DOI: 10.54254/2755-2721/2026.38751

peak pressure proxy are shown in Figure 2, and the medians with uncertainty intervals are shown in Figure 3.

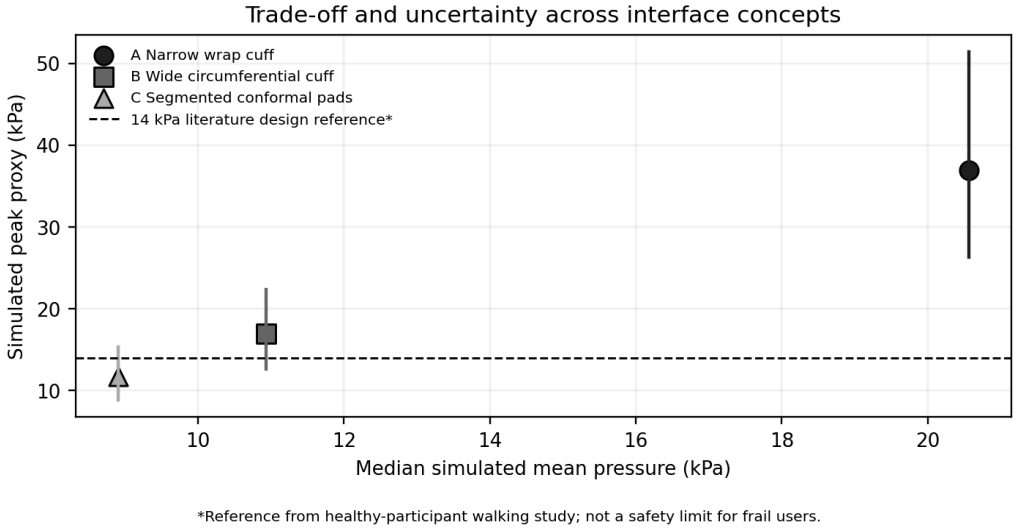


Figure 3. Simulated medians and uncertainty intervals for the three interface concepts. The dashed line marks a literature reference, not a clinical safety threshold

3.3. Sensitivity and design trade-offs

In our model, M and d determine the interface reaction through F = M/d. A larger assistive torque or a shorter distance between interfaces increases the reaction force. As φ decreases, the load-bearing area shrinks and mean pressure rises. K primarily affects the high-pressure tail of the peak proxy. Pad fit, edge lift, and retention strap preload therefore matter alongside nominal pad area.

The wide cuff has lower simulated mean pressure than the narrow cuff. A lower-limb compression study also found that a wider cuff could trigger discomfort at a lower pressure, with lower tolerance during walking than during standing [13]. Our mean pressure $\bar{p}$ describes a mechanical average and does not capture these physiological responses. Concept C uses segmented pads to carry the device reaction and a retention strap for positioning. Pressure sensing and slip tests are needed to determine whether this load path can be achieved in a prototype.

4. Product concept

A product concept called the Segmented Load-Bearing Knee Assist Frame is proposed. Its use by people with lower limb weakness who, after assessment by a rehabilitation professional, can still stand or take steps with some independence is envisaged. At the concept stage, use would be deferred for people unable to stand, people with severe osteoporosis that has not been assessed, marked sensory impairment, or damaged skin. Any effect on fall prevention or treatment of muscle atrophy would require separate evaluation. The side-view of the proposed structure is shown in Figure 4.

DOI: 10.54254/2755-2721/2026.38751

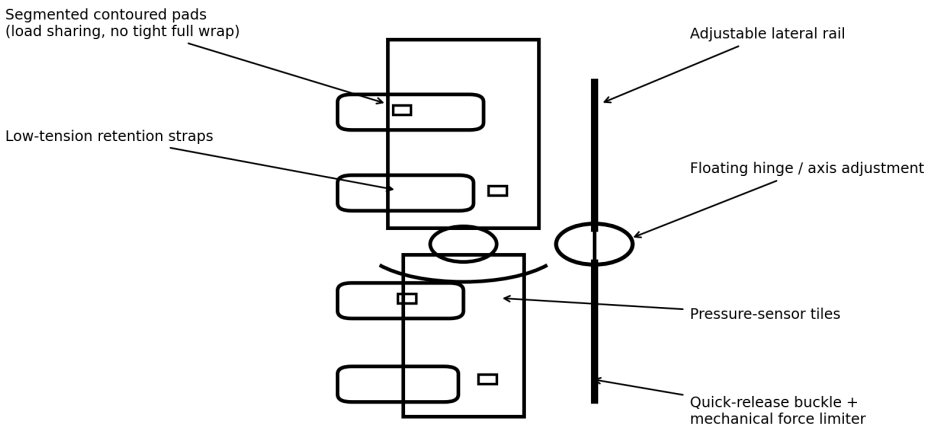


Figure 4. Side-view concept of the Segmented Load-Bearing Knee Assist Frame. The drawing illustrates a proposed structure. Dimensional design, bench testing, and human safety evaluation remain to be completed

Our concept includes two lateral rails, an adjustable floating knee hinge, contoured segmented pads for the thigh and shank, low-tension retention straps, pressure-sensing patches, and a mechanical quick-release buckle. The pads transfer the support reaction while leaving clearance over the front of the knee, where a rigid component could press on the patella. A small amount of hinge translation or rotation may reduce strap tension when the device axis does not align with the wearer's joint axis. Compliant elements help the pads conform and cushion the limb. Pressure sensors should not trigger abrupt changes in assistive output.

If proceeding to prototyping, the links could be made from adjustable aluminum extrusion or printed polymer and paired with soft foam or silicone pads and textile straps. Starting with a limb surrogate is recommended. Students and family members should not walk in a homemade device. Pressure sensors should record mean pressure, the 95th percentile, peak location, and pressure gradient. Markers or video can track movement of the frame relative to the limb. The quick release and force limiter should unload the device during power loss or misuse.

5. Verification plan and risk controls

A three-stage verification plan is recommended. First, calibrate the pressure sensors using a known area and weights, checking zero offset, linearity, hysteresis, and repeatability, then repeat the calibration on a curved surface. Second, compare pads statically on a limb model at the same torque and support spacing, recording pressure distribution, load, and slip. Third, conduct dynamic bench tests with a swing mechanism to represent standing, knee flexion, and stepping. Record when pressure peaks occur, how long they persist, any shear or slip, and any structural release. Repeat each condition at least five times and report the mean, standard deviation, sensor resolution, and failed trials.

A limb surrogate can reproduce mechanical phenomena such as geometric contact, interface pressure, and slip. Skin perfusion, muscle thickness, bone properties, pain sensation, and individual gait in older adults require other forms of evaluation. The surrogate results therefore support engineering screening at the bench stage. Any later usability study with people would require ethics approval and clinical supervision. It should include skin checks, discomfort reporting, assessment of

DOI: 10.54254/2755-2721/2026.38751

circulation and sensory risks, and clear stop criteria. ISO/TR 23482-1 calls for test methods to be selected through risk assessment. If the device is intended for medical or rehabilitation use, relevant regulations and standards will also need to be reviewed [14].

6. Discussion

Our model separates interface loading into two sources. The first is the reaction force produced when the exoskeleton supplies assistance. The second is the preload applied by the retention strap to limit slip. The first supports device function, while the second positions the frame. Treating them separately lets us examine the compression associated with strap preload. The segmented pads are intended to carry the support load while the textile straps maintain position. Slip and shear testing will show whether these load paths can remain distinct in a prototype.

Most pressure tolerance studies have involved healthy volunteers, specific cuffs, and prescribed walking tasks. Older adults with muscle atrophy, sensory loss, circulatory problems, or osteoporosis may differ from those samples. 14 kPa is used as a reference for comparing concepts in the figures. Skin interface pressure and fracture risk are different outcomes. The latter requires separate assessment of bone health, structural device loads, and fall scenarios.

Soft-tissue mechanics are approximated using an effective contact fraction and a concentration factor, and contact is represented as a two-dimensional synthetic pressure field. The current model does not include nonlinear soft-tissue properties, frictional contact, internal tissue stress, or correlations among parameters for a given wearer. The simulation intervals therefore describe uncertainty under the input assumptions used here. If bench data become available, pressure arrays and load cells can be used to calibrate the parameters and then a finite element contact model or an individualized geometric model can be developed.

This is a modeling and simulation study. Human participants were not recruited and human or animal data were not collected. All figures and statistics were generated from the simulation parameters reported here. If limb-surrogate tests are conducted, material batches, measurement procedures, and raw data will be reported. Any human study will require an ethics approval number and a description of the informed consent process.

7. Conclusions

A simplified model linking knee assistive torque to interface reaction force, effective contact area, and a local pressure proxy was developed, then 10,000 Monte Carlo trials were run for three strap and pad concepts. Under the parameters used here, the segmented compliant pads produced lower simulated mean pressure and peak proxy values. This result follows mainly from their higher effective contact fraction and lower retention preload. The present findings come from a computational model. Actual wearing performance will require prototype, bench, and later human evaluation.

Based on this analysis, a product concept with lateral rails, a floating knee hinge, segmented compliant load-bearing pads, low-tension retention straps, pressure monitoring patches, and a mechanical quick release is proposed. Calibrating the sensors and testing the concept on a limb surrogate first, with particular attention to peak pressure, pressure duration, slip, and repeatability, is recommended. Given muscle atrophy and possible bone fragility, wearable settings for people should be determined through professional assessment and validation studies.

DOI: 10.54254/2755-2721/2026.38751

References

[1] De Rossi, S. M. M., Vitiello, N., Lenzi, T., Ronsse, R., Koopman, B., Persichetti, A., Vecchi, F., Ijspeert, A. J., van der Kooij, H., & Carrozza, M. C. (2011). Sensing pressure distribution on a lower-limb exoskeleton physical human-machine interface. *Sensors, 11*, 207–227. https://doi.org/10.3390/s110100207.

[2] Tamez-Duque, J., Cobian-Ugalde, R., Kilicarslan, A., Venkatakrishnan, A., Soto, R., & Contreras-Vidal, J. L. (2015). Real-time strap pressure sensor system for powered exoskeletons. *Sensors, 15*, 4550–4563. https://doi.org/10.3390/s150204550.

[3] Massardi, S., Rodriguez-Cianca, D., Pinto-Fernández, D., Moreno, J. C., Lancini, M., & Torricelli, D. (2022). Characterization and evaluation of human-exoskeleton interaction dynamics: A review. *Sensors, 22*, 3993. https://doi.org/10.3390/s22113993.

[4] Shushtari, M., et al. (2024). Human-exoskeleton interaction portrait. *Journal of NeuroEngineering and Rehabilitation, 21*, 133. https://doi.org/10.1186/s12984-024-01447-1.

[5] Kermavnar, T., O'Sullivan, K. J., Casey, V., de Eyto, A., & O'Sullivan, L. W. (2020). Circumferential tissue compression at the lower limb during walking, and its effect on discomfort, pain and tissue oxygenation: Application to soft exoskeleton design. *Applied Ergonomics, 86*, 103093. https://doi.org/10.1016/j.apergo.2020.103093.

[6] Kermavnar, T., Power, V., de Eyto, A., & O'Sullivan, L. Cuff pressure algometry in patients with chronic pain as guidance for circumferential tissue compression for wearable soft exoskeletons: A systematic review. *Soft Robotics, 5*, 497–511. https://doi.org/10.1089/soro.2017.0088.

[7] Armitage, L., Turner, S., & Sreenivasa, M. Human-device interface pressure measurement in prosthetic, orthotic and exoskeleton applications: A systematic review. *Medical Engineering & Physics, 97*, 56–69. https://doi.org/10.1016/j.medengphy.2021.09.008.

[8] Kermavnar, T., O'Sullivan, K. J., de Eyto, A., & O'Sullivan, L. W. Relationship between interface pressures and pneumatic cuff inflation pressure at different assessment sites of the lower limb to aid soft exoskeleton design. *Human Factors, 63*, 101–114. https://doi.org/10.1177/0018720820908758.

[9] Sanchez-Villamañan, M. C., Gonzalez-Vargas, J., Torricelli, D., Moreno, J. C., & Pons, J. L. Compliant lower limb exoskeletons: A comprehensive review on mechanical design principles. *Journal of NeuroEngineering and Rehabilitation, 16*, 55. https://doi.org/10.1186/s12984-019-0517-9.

[10] Kermavnar, T., O'Sullivan, K. J., de Eyto, A., & O'Sullivan, L. W. Discomfort/pain and tissue oxygenation at the lower limb during circumferential compression: Application to soft exoskeleton design. *Human Factors, 62*, 470–484. https://doi.org/10.1177/0018720819892098.

[11] Bessler, J., Prange-Lasonder, G. B., Schaake, L., Saenz, J. F., Bidard, C., Fassi, I., Valori, M., Lassen, A. B., & Buurke, J. H. (2021). Safety assessment of rehabilitation robots: A review identifying safety skills and current knowledge gaps. *Frontiers in Robotics and AI, 8*, 602878. https://doi.org/10.3389/frobt.2021.602878.

[12] International Organization for Standardization. (2020). ISO/TR 23482-1:2020 robotics-application of ISO 13482-part 1: Safety-related test methods. ISO.

[13] Wang, T., et al. (2022). A review on the rehabilitation exoskeletons for the lower limbs of the elderly and the disabled. *Electronics, 11*, 388. https://doi.org/10.3390/electronics11030388.

[14] Lowe, B. D., Billotte, W. G., & Peterson, D. R. (2019). ASTM F48 formation and standards for industrial exoskeletons and exosuits. *IISE Transactions on Occupational Ergonomics and Human Factors, 7*, 230–236. https://doi.org/10.1080/24725838.2019.1579769.